University Library

MINERVA ACCESS

A gateway to Melbourne's research publications

Minerva Access is the Institutional Repository of The University of Melbourne

Author/s:
Arsic, N;Gadea, G;Lagerqvist, EL;Bußon, M;Cahuzac, N;Brock, C;Hollande, F;Gire, V;Pannequin, J;Roux, P

Title:
The p53 isoform Δ133p53β promotes cancer stem cell potential

Date:
2015-01-01

Citation:
Arsic, N., Gadea, G., Lagerqvist, E. L., Bußon, M., Cahuzac, N., Brock, C., Hollande, F., Gire, V., Pannequin, J. & Roux, P. (2015). The p53 isoform Δ133p53β promotes cancer stem cell potential. Stem Cell Reports, 4 (4), pp.531-540. https://doi.org/10.1016/j.stemcr.2015.02.001.

Persistent Link:
https://hdl.handle.net/11343/240585

License:
CC BY-NC-ND

Stem Cell Reports
Report
OPEN ACCESS

The p53 Isoform Δ133p53β Promotes Cancer Stem Cell Potential

Nikola Arsic,[1,7] Gilles Gadea,[1,7] E. Louise Lagerqvist,[2] Muriel Busson,[3] Nathalie Cahuzac,[4] Carsten Brock,[5] Frederic Hollande,[6] Veronique Gire,[1] Julie Pannequin,[2] and Pierre Roux[1,*]
[1]Centre National de la Recherche Scientifique, UMR 5237, Centre de Recherche en Biochimie Macromoléculaire, Université Montpellier, 1919 route de Mende, 34293 Montpellier Cedex 5, France
[2]Centre National de la Recherche Scientifique, UMR5203, Institut de Génomique Fonctionnelle, Institut National de la Santé et de la Recherche Médicale, U661, Université Montpellier, route de Cardonille, 34094 Montpellier, France
[3]Plateforme Imagerie du Petit Animal de Montpellier (IPAM), Institut de Recherche en Cancérologie de Montpellier Inserm U896, Université Montpellier, ICM Val d'Aurelle Campus Val d'Aurelle, 208 Rue des Apothicaires, 34298 Montpellier Cedex 5, France
[4]Eurobiodev, 2040 avenue du Père Soulas, 34090 Montpellier, France
[5]Eurofins Cerep, Le bois L'Evèque, 86600 Celle L'Evescault, France
[6]Department of Pathology, University of Melbourne, Parkville, VIC 3010, Australia
[7]Co-first author
*Correspondence: pierre.roux@crbm.cnrs.fr
http://dx.doi.org/10.1016/j.stemcr.2015.02.001
This is an open access article under the CC BY-NC-ND license (http://creativecommons.org/licenses/by-nc-nd/4.0/).

SUMMARY

Cancer stem cells (CSC) are responsible for cancer chemoresistance and metastasis formation. Here we report that Δ133p53β, a *TP53* splice variant, enhanced cancer cell stemness in MCF-7 breast cancer cells, while its depletion reduced it. Δ133p53β stimulated the expression of the key pluripotency factors *SOX2*, *OCT3/4*, and *NANOG*. Similarly, in highly metastatic breast cancer cells, aggressiveness was coupled with enhanced CSC potential and Δ133p53β expression. Like in MCF-7 cells, *SOX2*, *OCT3/4*, and *NANOG* expression were positively regulated by Δ133p53β in these cells. Finally, treatment of MCF-7 cells with etoposide, a cytotoxic anti-cancer drug, increased CSC formation and *SOX2*, *OCT3/4*, and *NANOG* expression via Δ133p53, thus potentially increasing the risk of cancer recurrence. Our findings show that Δ133p53β supports CSC potential. Moreover, they indicate that the *TP53* gene, which is considered a major tumor suppressor gene, also acts as an oncogene via the Δ133p53β isoform.

INTRODUCTION

The p53 functions are ubiquitously altered in cancer cells by mutations/perturbation of its signaling pathways, and loss of p53 activity is a prerequisite for cancer development. Mutant p53 is thought to play a pivotal role in promoting invasion, favoring cancer cell exit from the primary tumor site and dissemination, ultimately leading to metastasis formation (Gadea et al., 2007; Muller et al., 2009; Roger et al., 2010; Vinot et al., 2008).

Recent reports have documented a p53 role in stem cell homeostasis and pluripotency. Wild-type (WT) p53 counteracts somatic cell reprogramming (Hong et al., 2009; Kawamura et al., 2009; Liu et al., 2009; Utikal et al., 2009), whereas mutant p53 stimulates induced pluripotent stem (iPS) cell formation (Sarig et al., 2010). Depletion of p53 significantly increases cell reprogramming efficacy and facilitates iPS cell generation (Kawamura et al., 2009). Consequently, p53 might be considered as the guardian of the genome and also of reprogramming.

All these functions are associated with full-length p53 (i.e., the TAp53α isoform). However, the *TP53* gene encodes at least 12 different physiological isoforms (TAp53 [α, β, and γ], Δ40p53 [α, β, and γ], Δ133p53 [α, β, and γ], and Δ160p53 [α, β, and γ]) (Bourdon, 2007) via several mechanisms: alternative promoters (the TA and Δ133 isoforms), alternative intron splicing (intron 2: Δ40 isoforms and intron 9: α, β, and γ isoforms), and alternative translational initiation sites (Δ40 and Δ160 isoforms). The TAp53α isoform is the best described and classically mentioned in the literature as p53. Basically, p53 isoforms can be divided into two groups as follows: (1) long isoforms that contain the transactivation domain (TA and Δ40), and (2) short isoforms without the transactivation domain (Δ133 and Δ160). Furthermore, the β and γ isoforms do not contain the canonical C-terminal oligomerization domain, but an additional domain with unknown function(s) (Khoury and Bourdon, 2011).

The p53 isoforms modify p53 transcriptional activity in many processes, such as cell-cycle progression, programmed cell death, replicative senescence, cell differentiation, viral replication, and angiogenesis (Aoubala et al., 2011; Bernard et al., 2013; Bourdon et al., 2005; Marcel et al., 2012; Terrier et al., 2011, 2012). Importantly, p53 isoforms are specifically deregulated in human tumors (Machado-Silva et al., 2010). However, the functions of p53 isoforms in cancer stem cell (CSC) homeostasis have never been explored.

Here, we show that the Δ133p53β isoform is specifically involved in promoting cancer cell stemness. Overexpression of Δ133p53β in human breast cancer cell lines stimulated mammosphere formation and the expression of key

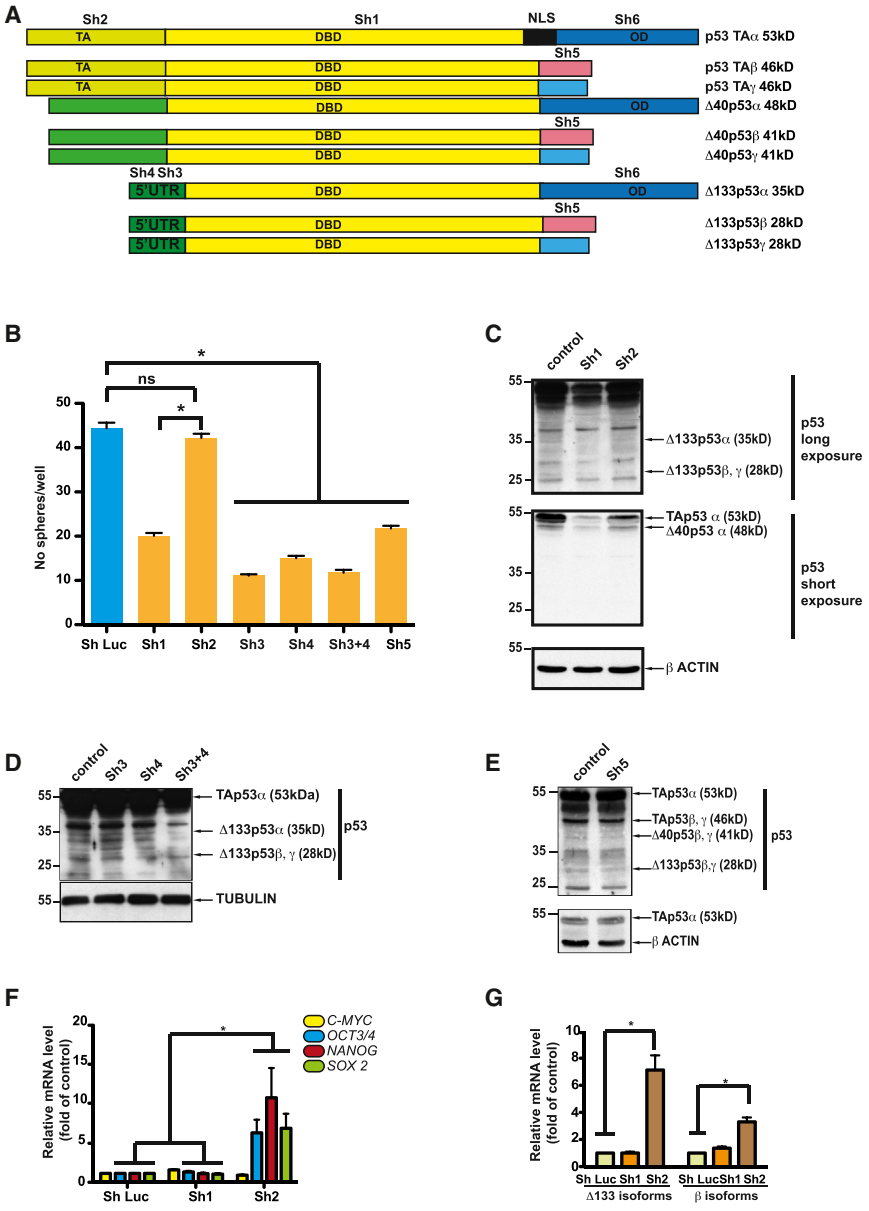


Figure 1. Selective Depletion of p53 Isoforms Affects the Sphere-Forming Ability of MCF-7 Cells

(A) Schematic representation of p53 isoforms with the targets of the different shRNAs (Sh) used in this study. The calculated molecular weights of the different isoforms are indicated.

(B) Mammosphere quantification in MCF-7 cells after transduction of Sh1, Sh2, Sh3, Sh4, and Sh5 (n = 3 independent experiments).

(C–E) Western blot analysis of p53 isoform depletion in the corresponding cells.

(F and G) The qRT-PCR quantification of the expression levels of *C-MYC*, *SOX2*, *OCT3/4*, and *NANOG* (F) as well as of Δ133p53 and p53 β isoforms (G) after transduction with Sh1 and Sh2 (n = 4 independent experiments).

pluripotency and stemness regulators (*SOX2*, *OCT3/4*, and *NANOG* and *CD24/CD44*), but not *C-MYC*. Furthermore, using MDA-MB-231-based cell lines, we show that increased expression of Δ133p53 isoforms correlates with the increased metastatic potential and with mammosphere formation. Finally, incubation of MCF-7 and MDA-MB-231 cells with the anti-cancer drug etoposide also promoted cell stemness in a Δ133p53-dependent manner. Our results demonstrate that short p53 isoforms positively regulate CSC potential regardless of any p53 mutation. Consequently, WT *TP53*, which is considered a tumor suppressor gene, also can act as an oncogene through Δ133p53β expression.

RESULTS

Changes in the Expression of p53 Isoforms Affect Mammosphere Formation

To study the role of the different p53 isoforms in CSC potential, we designed small hairpin RNAs (shRNAs) (Sh) that selectively silence specific groups of isoforms (Figure 1A; Table S1). Briefly, Sh1 knocks down all p53 isoforms, while Sh2 targets the long TAp53 (*trans*-activating) and Δ40p53 isoforms. Sh3 and Sh4 target the 5′ UTR of the Δ133 isoforms (α, β, and γ), and Sh5 and Sh6 respectively target the 3′ end of the β and α isoforms.

First, we tested the ability of MCF-7 cells to form mammospheres, an assay widely used to assess CSC potential in vitro. Silencing of all p53 isoforms (with Sh1) resulted in a significant reduction of mammosphere formation compared to control cells, while knockdown of the TAp53 and Δ40p53 isoforms (Sh2) had no effect (Figures 1B and 1C). In parallel we measured the mRNA (Figure 1F) and protein (Figure S1A) expression of C-MYC, SOX 2, OCT 3/4, and NANOG, which are key regulators of cell pluripotency. TAp53 and Δ40p53 (Sh2) silencing resulted in increased expression of OCT 3/4, NANOG, and SOX 2, but not of C-MYC, while depletion of all p53 isoforms (Sh1) had no effect. Moreover, depletion of TAp53 and Δ40p53 (Sh2) increased the expression of the Δ133 isoforms (Figure 1G).

These results suggest that the CSC potential in MCF-7 cells is not only regulated by TAp53α, which previously was identified as a suppressor of stemness. To investigate this hypothesis, we depleted all Δ133 isoforms using two different shRNAs (Sh3 and 4). Both shRNAs, used either alone or in combination, significantly reduced mammosphere formation in MCF-7 cells, suggesting that these isoforms are key regulators of the CSC potential (Figures 1B and 1D). Accordingly, OCT3/4, NANOG, and SOX2 were significantly downregulated in Δ133-isoform-silenced cells (Figure S1A). Again C-MYC expression was not affected. We then evaluated the effect of β and α isoform silencing. Mammosphere formation was significantly reduced in cells in which β isoforms where knocked down (Sh5; Figure 1B). Silencing of all α isoforms (Sh6) did not affect mammosphere formation (Sh6; Figures S1B and S1C). Altogether these findings suggest that Δ133p53 (α, β, and γ) isoforms are involved in regulating CSC potential in MCF-7 cells.

The Δ133p53β Isoform Promotes CSC Potential in MCF-7 Cells

Indeed, mammosphere formation was significantly increased in MCF-7 cells that expressed only the Δ133p53β and Δ133p53γ isoforms following concomitant transduction with Sh2 and Sh6 (Figures 2A and 2B). To confirm that sphere increase was indicative of the CSC phenotype, we analyzed the proportion of $CD44^+/CD24^-$ cells, because this subpopulation of cancer cells are considered to have CSC properties. Similar to mammosphere formation variations, the proportion of $CD44^+/CD24^-$ cells was not affected by TAp53 and Δ40p53 isoform silencing with Sh2, whereas it was increased by co-transduction of Sh2 and Sh6 (Figure 2C).

To determine the specific contribution of the Δ133p53 (β and γ) isoforms in promoting mammosphere formation, we overexpressed them separately. In agreement with the previous results, Δ133p53β overexpression significantly promoted mammosphere formation, while γ isoform overexpression had a milder effect (Figures 2D and S2). Moreover, Δ133p53β overexpression resulted in a significant increase of *SOX2*, *NANOG*, and *OCT3/4* expression, but not of *C-MYC* (Figure 2E). In addition, mammosphere formation by Δ133p53β-expressing cells was higher after harvesting and re-plating of primary mammospheres, which is considered the gold standard experiment to challenge the CSC phenotype in vitro (Figure 2F).

Finally, to confirm the role of the Δ133p53β isoform in promoting CSC potential in MCF-7 cells, we overexpressed a Sh1-resistant Δ133p53β isoform in MCF-7 cells in which all p53 isoforms had been knocked down with Sh1. As expected, expression of Sh1-resistant Δ133p53β rescued mammosphere formation (Figure 2G). These results indicate that the Δ133p53β isoform positively regulates CSC potential in MCF-7 breast cancer cells.

High Δ133p53 Levels Correlate with Increased Metastatic Capacity and Mammosphere Formation

Increasing evidence suggests that the CSC phenotype and metastasis development are closely linked. We therefore asked whether the metastatic capacity of breast cancer cells was coupled to their CSC potential and Δ133p53 isoform expression. To this end, we used MDA-MB-231 D3H2LN cells, which can generate, at low frequency, lung metastasis when transplanted in immunodeficient mice, to derive the highly cancer-prone and very metastatic C3LND cell line (Figures S3A and S3B). When this line was used for orthotopic transplantation experiments in nude mice, metastasis detection time was reduced from 82 days (with parental D3H2LN cells) to 20 days, and lung metastases were detected in all transplanted animals (Figure S3C). Although primary tumor growth was comparable in both cell lines (Figure S3D), metastasis development was significantly accelerated in the C3LND cells, as indicated by bioluminescence quantification (Figure S3E).

Evaluation of mammosphere formation in D3H2LN and C3LND cells showed that C3LND cells formed two times more mammospheres (Figure 3A). Similarly, Δ133p53 isoform expression was 3-fold higher and *OCT3/4*, *NANOG*, and *SOX2* levels were 2- to 3-fold higher in C3LND (Figures 3B and 3C). *C-MYC* expression was comparable in the two cells lines. We then asked whether pluripotency factor expression could be affected by changes in Δ133p53 expression. Overexpression of Δ133p53β in D3H2LN cells resulted in a significant increase of *OCT3/4*, *NANOG*, and *SOX2* expression, whereas *C-MYC* level was not affected, consistent with data in MCF-7 cells (Figures 3D and 3E). Similar results were obtained in C3LND cells (Figure S3F). In complete agreement with observations in MCF-7, Δ133p53β overexpression in D3H2LN cells resulted in a significant increase of mammosphere formation (Figure 3F).

Conversely, knockdown of the Δ133p53 isoforms with Sh3 in C3LND cells led to a significant reduction of sphere

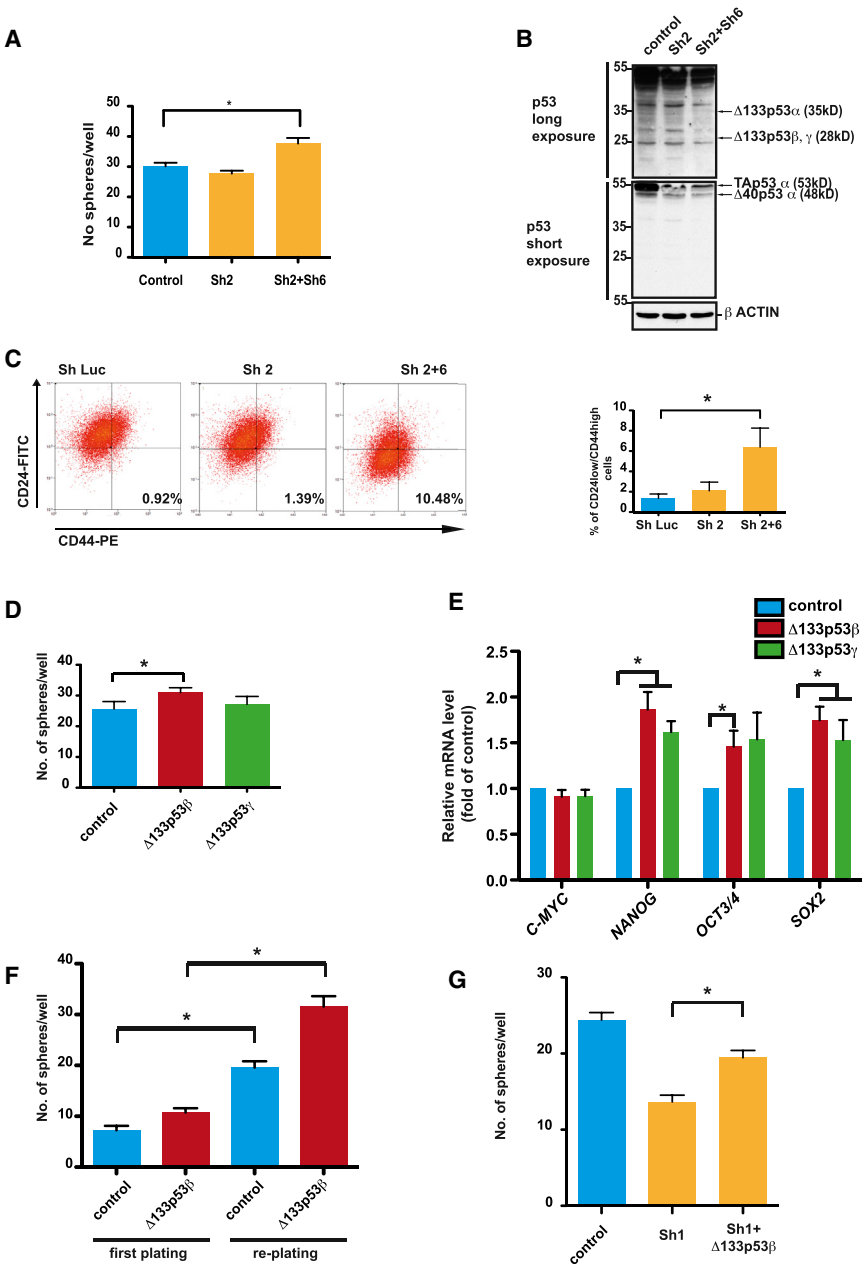


Figure 2. The Isoform Δ133p53β Promotes CSC Potential in MCF-7 Cells

(A and B) Mammosphere quantification in MCF-7 cells after silencing with Sh2 (shRNAs against the TA and Δ40 isoforms) or with Sh2 and Sh6 (against the 3′ end of the α isoforms) (A) and western blot analysis to confirm p53 depletion in the corresponding cell cultures (B) (n = 3 independent experiments).

(C) Representative fluorescence-activated cell sorting (FACS) dot blots for the double labeling of CD24 and CD44 in MCF-7 transduced with Sh Luc (Control), Sh2, or Sh2 + 6.

(D and E) Mammosphere quantification in MCF-7 cells after Δ133p53β or γ overexpression (D) and qRT-PCR analysis of *C-MYC*, *SOX2*, *OCT3/4*, and *NANOG* (E) expression in the corresponding cells (n = 4 independent experiments).

(F) Mammosphere quantification in MCF-7 cells that overexpress Δ133p53β after harvesting and re-plating of the primary mammospheres (n = 4 independent experiments).

(G) Mammosphere quantification in MCF-7 cells in which all p53 isoforms have been silenced with Sh1 and after expression in the same cells of Sh1-resistant Δ133p53β (n = 3 independent experiments).

formation; a marked decrease of *OCT3/4*, *NANOG*, and *SOX2* expression; and a small increase of *C-MYC* level (Figures 3G–3I), whereas Δ133p53β transduction increased them (Figure S3F). In agreement, Sh3 transduction decreased the proportion of $CD44^{+}/CD24^{-}$ cells (Figure 3J). Finally, after intracardiac injection in athymic mice, Sh3-transduced C3LND cells were less prone to metastasize to distant sites compared to control cells (Figures 3K, 3L, S3G, and S3L).

In summary, the more metastatic C3LND cell line is characterized by higher CSC potential, as indicated by mammosphere formation and increased Δ133p53 as well as *OCT3/4*, *NANOG*, and *SOX2* (but not *C-MYC*) expression compared to the parental D3H2LN cell line. Δ133p53 overexpression increases the pluripotency potential of D3H2LN cells, while its knockdown produces the opposite effect and a marked reduction of their metastatic potential when grafted in mice. Altogether these data suggest that the Δ133p53β isoform specifically regulates CSC activity and metastasis formation through modulation of the expression of key cell pluripotency and reprogramming factors (i.e., *OCT3/4*, *NANOG*, and *SOX2*).

Chemotherapy Treatment of Breast Cancer Cell Lines Upregulates the Expression of Δ133p53 Isoforms and Activates Key Reprogramming Genes

Topoisomerase II inhibitors (etoposide-VP16 and doxorubicin) are frequently used as adjuvant chemotherapy treatment for several cancer types alone or in combination with other drugs (cisplatin most frequently). Topoisomerase II inhibitors induce double-strand DNA breaks, a genotoxic stress that strongly activates p53 signaling. Upregulation of TAp53 should be beneficial due to its ability to induce cell-cycle arrest, apoptosis, and to negatively regulate cell reprogramming. We thus assessed whether etoposide could affect Δ133p53 expression and CSC potential in breast cancer cell lines. Increasing concentrations of etoposide resulted in TAp53α stabilization in MCF-7. As expected, p21 expression (positively regulated by p53) was increased, whereas C-MYC expression (negatively regulated by p53) was reduced (Figure 4A), as also confirmed by qRT-PCR quantification (Figure 4B). Moreover, qRT-PCR and western blot analysis showed that, upon etoposide treatment, Δ133p53 isoforms (Figures 4C and 4D) as well as *OCT3/4*, *NANOG*, and *SOX2* (Figure 4E) were strongly upregulated in a dose-dependent manner. This last result is particularly intriguing because TAp53α, which is considered as a negative regulator of pluripotency/reprogramming genes, is stabilized and transcriptionally active.

To determine whether *OCT3/4*, *NANOG*, and *SOX2* upregulation in this condition required Δ133p53 expression, we transduced MCF-7 cells with Sh3 to specifically knock them down. *OCT3/4*, *NANOG*, and *SOX2* expression were reduced in both etoposide-treated and untreated cells following Δ133p53 silencing (Figure 4F), confirming the specific role of Δ133p53 isoforms in the regulation of genes involved in cell pluripotency/reprogramming.

Finally, we evaluated the effect of etoposide treatment on mammosphere formation in Sh2-transduced MCF-7 cells. Etoposide treatment in control cells (active TAp53) significantly reduced mammosphere formation, whereas it did not have any significant effect in Sh2-transduced cells (Figure 4G). Moreover, Δ133p53 level was correlated with the expression of reprogramming genes (Figures 4H and 4I). These data indicate that TAp53 and Δ133p53β have an antagonistic action in sphere formation.

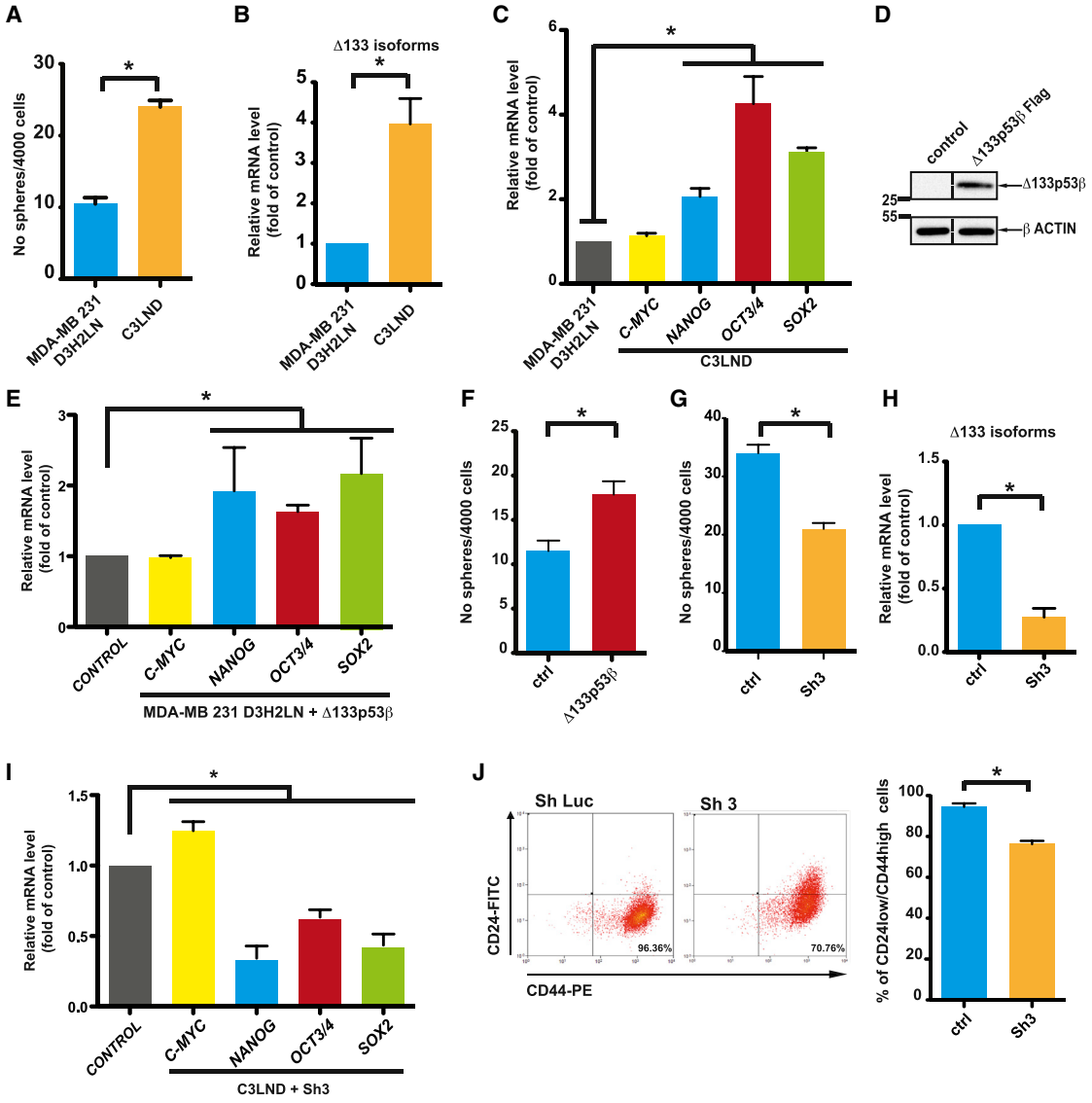
We then evaluated the effects of etoposide treatment in MDA-MB-231 D3H2LN cells that harbor the p53 R280K mutation and correspond to a triple-negative breast cancer type. This mutation is present in TAp53 and also in Δ133p53 isoforms. Incubation with increasing concentrations of etoposide did not affect TAp53 expression, and p21 expression was only weakly increased (Figure S4A). This effect of mutant p53 protein on p21 expression already has been described in the literature (Bieging et al., 2014). Interestingly, C-MYC expression was significantly downregulated (Figures S4A and S4B). The expression of Δ133p53 isoforms was upregulated (Figures S4A and S4C), but not in a dose-dependent manner, as observed in MCF-7 cells. Similarly, the expression of *NANOG*, *SOX2*, and *OCT3/4* (Figure S4D) also was upregulated following incubation with etoposide, like for Δ133p53 isoforms.

These data suggest that, in human breast cancer cells, the topoisomerase II inhibitor etoposide increases Δ133p53 expression, resulting in the activation of the reprogramming genes *NANOG*, *SOX2*, and *OCT3/4*.

DISCUSSION

In this work, by modulating p53 isoform expression in breast cancer cell lines, we show that Δ133p53 isoforms have a role in regulating their stemness potential. Surprisingly, depletion of all p53 isoforms in MCF-7 cells significantly reduced mammosphere formation (a hallmark of CSC potential), although previous reports indicate that TAp53α hinders cell reprogramming. Conversely, selective depletion of TAp53 and Δ40p53 isoforms with the Sh2 shRNA did not affect mammosphere formation, suggesting that Δ133p53 isoforms are responsible for this activity. We then confirmed this hypothesis by showing that mammosphere formation was strongly reduced upon knockdown of these small isoforms (Figure 1). Similarly, depletion of the β isoforms had a deleterious effect on the capacity of MCF-7 cell to form mammospheres, while depletion of the α isoforms did not have any effect. Moreover, all changes in p53 isoform expression, particularly Δ133p53, were associated with variations in the expression of *SOX2*, *OCT3/4*, and *NANOG*, key cell pluripotency/reprogramming genes, but not of *C-MYC* (Figures 1 and 2). Furthermore, the finding that Δ133p53β isoform specifically promoted mammosphere formation and increased the proportion of $CD44^{+}/CD24^{-}$ cells indicates that this isoform positively regulates CSC potential in MCF-7 breast cancer cells. Indeed, our data show that Δ133p53β expression positively correlates with *SOX2*, *OCT3/4*, and *NANOG* expression, genes responsible for cell pluripotency induction and maintenance (Figure 2). Finally, using a breast cell model of tumor aggressiveness, we show that higher metastatic potential and chemoresistance are coupled with increased expression of the Δ133p53 isoforms, CSC stemness, and increased expression of key pluripotency/reprogramming genes (Figures 3 and 4).

Importantly, our results show that TAp53 (α, β, and γ) silencing does not affect CSC formation, whereas Δ133p53 (α, β, and γ) silencing does, indicating that the



(legend on next page)

CSC potential is mainly regulated by Δ133p53 activity rather than by TAp53.These findings challenge the prominent role of full-length p53 (TAp53α) in CSC regulation and clearly indicate that most of the p53-mediated regulation of the CSC potential is via the short p53 isoforms.

While the role of TAp53 (full-length p53) in CSC formation has been largely documented, the role of other p53 isoforms is still poorly described. The isoform Δ40p53, a highly expressed isoform in embryonic stem cells, has been proposed to control pluripotency by maintaining TAp53 in an inactive form (Ungewitter and Scrable, 2010). Thus, the p53 stemness response could be determined by the composition of the complexes formed by different p53 isoforms with synergistic or antagonistic activity. Our data indicate that Δ133p53β effects are mediated through regulation of *SOX2*, *OCT3/4*, and *NANOG* expression. As TAp53 is a negative regulator of these genes, it is tempting to suggest a dominant-negative effect of the Δ133p53β isoform as a mechanism of action. However, Δ133p53β did not affect the expression of *C-MYC*, another TAp53-regulated gene. Thus, we cannot exclude the possibility of gain-of-function properties for the small isoforms relative to the long ones, as suggested by etoposide treatment experiments. A similar mechanism has been proposed already for the mutated p53 variants that facilitate somatic cell reprogramming and increase the malignant potential of reprogrammed cells (Sarig et al., 2010). Gain-of-function properties of p53 isoforms also are involved in the regulation of some aspects of cell-cycle progression (Olivares-Illana and Fåhraeus, 2010). In any case, these two mechanisms (dominant-negative and gain-of-function effects) are not mutually exclusive and further studies are needed to evaluate their contribution.

In summary, our study shows that Δ133p53β plays a critical role in supporting the CSC potential of breast cancer cells. Mutations of *TP53* are considered the main mechanism for inhibiting its tumor suppressor activity. Here, we demonstrate that p53 mutations are not necessary to block p53 tumor suppressor activity, because expression of specific p53 isoforms, particularly Δ133p53β, is sufficient to increase CSC activity. Our study challenges the paradigm that *TP53* always acts as a tumor suppressor by showing that Δ133p53β antagonizes TAp53α to promote CSC potential.

EXPERIMENTAL PROCEDURES

Detailed Experimental Procedures are available in the Supplemental Information posted online with this paper.

MDA-MB-231 C3LND Cell Line Establishment

The C3LND cell line was derived from distant metastases of the MDA-MB-231-luc-D3H2LN cell line after two in vivo passages in nude mice. Briefly, 1×10^6 cells per animal were resuspended in sterile PBS for intracardiac injection (first cycle of enrichment) or in 50% Matrigel (BD Biosciences) for injection in the lower left mammary fat pad (second cycle of enrichment) of athymic nude mice (Hsd:Athymic Nude-Foxn1, Harlan). Tumor progression and time to metastasis were followed weekly by whole-body bioluminescence imaging. Invaded organs were then resected and tumor cells isolated and propagated in vitro.

Statistical Analysis

All data are presented as the arithmetic mean ± SEM. Statistical analyses were performed using the non-parametric Mann-Whitney t test with the Prism software (GraphPad).

Figure 3. Evaluation of the CSC Features of the MDA-MB-231 D3H2LN and C3LND Cell Lines

(A) Mammosphere quantification in the modestly metastatic, parental MDA-MB-231 D3H2LN and the derived, highly metastatic C3LND cell lines (n = 3 independent experiments).

(B) The qRT-PCR analysis of Δ133p53 isoform expression in MDA-MB-231 D3H2LN and C3LND cells (n = 4 independent experiments).

(C) The qRT-PCR quantification of *C-MYC*, *OCT3/4*, *NANOG*, and *SOX2* expression in MDA-MB-231 D3H2LN and C3LND cells (n = 4 independent experiments).

(D) Western blot analysis of Δ133p53β-Flag transduced in MDA-MB-231 D3H2LN cells (Flag antibody).

(E) The qRT-PCR analysis of *C-MYC*, *OCT3/4*, *NANOG*, and *SOX2* expression in MDA-MB-231 D3H2LN cells after Δ133p53β overexpression (n = 4 independent experiments).

(F) Mammosphere quantification in MDA-MB-231 D3H2LN cells that overexpress Δ133p53β (n = 3 independent experiments).

(G) Mammosphere quantification in MDA-MB-231 C3LND transduced with Sh3 (n = 3 independent experiments).

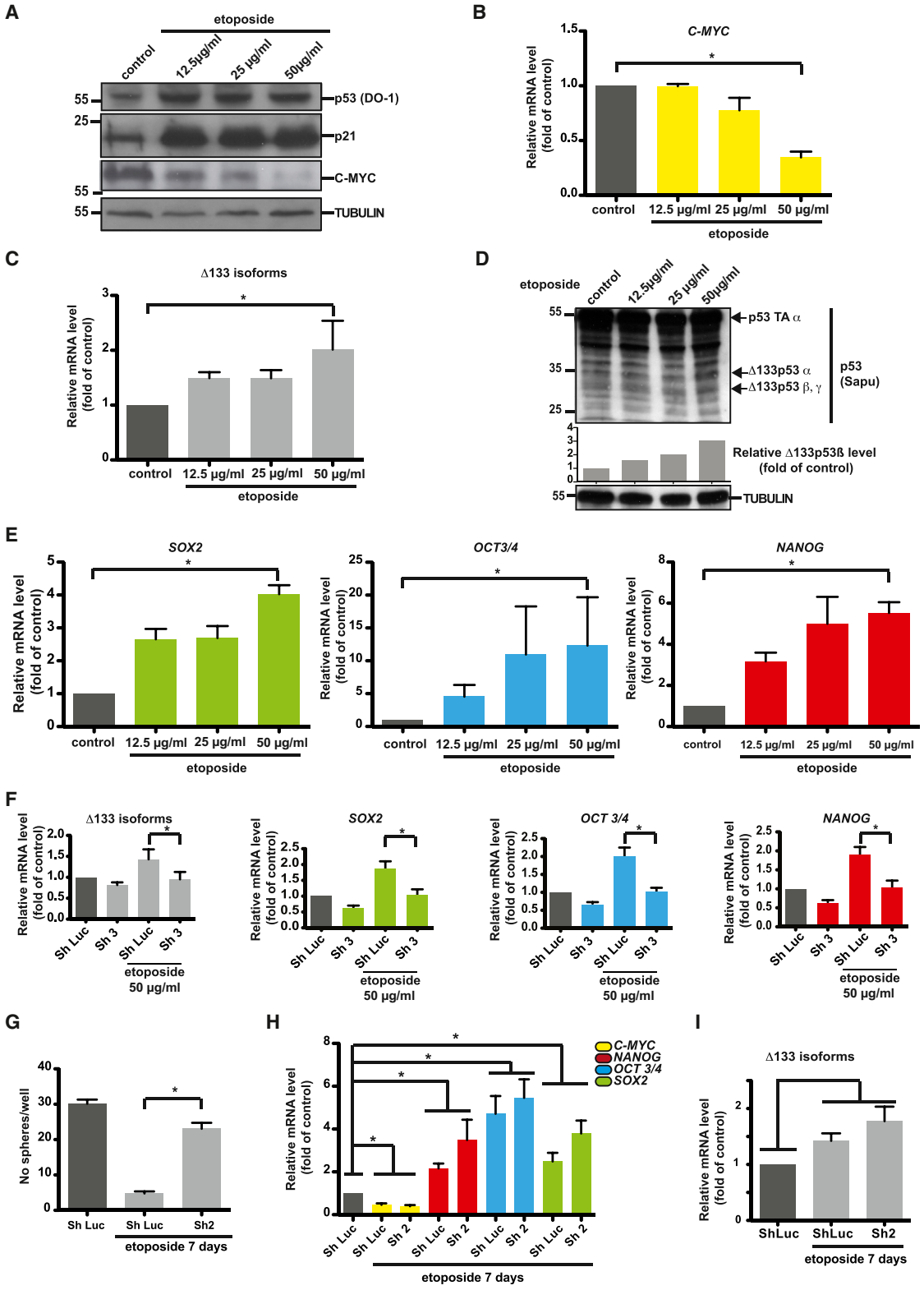
(H) The qRT-PCR analysis of Δ133p53 isoform expression in MDA-MB-231 C3LND transduced with Sh3 (n = 3 independent experiments).

(I) The qRT-PCR quantification of *C-MYC*, *OCT3/4*, *NANOG*, and *SOX2* expression in MDA-MB-231 C3LND cells transduced with Sh3 (n = 4 independent experiments).

(J) Representative FACS dot plots for the double labeling of CD44 and CD24 in MDA-MB-231 C3LND transduced with Sh Luc (Control) or Sh3 (n = 3 independent experiments).

(K) Bioluminescence ventral images of mice injected with MDA-MB-231 C3LND cells transduced with Sh3 or control. Pseudocolor scale bars show relative changes at metastatic sites.

(L) Quantification of distant metastasis in brain and femur using bioluminescence imaging (n = 7/5) 25 days after the implantation. Bars represent mean ± SEM of biological replicates.



(legend on next page)

In Vivo Experiments

All in vivo experiments were performed in compliance with the French regulations and ethical guidelines for experimental animal studies in an accredited establishment (Agreement No. C34-172-27).

SUPPLEMENTAL INFORMATION

Supplemental Information includes Supplemental Experimental Procedures, four figures, and one table and can be found with this article online at http://dx.doi.org/10.1016/j.stemcr.2015.02.001.

AUTHOR CONTRIBUTIONS

P.R., N.A., and G.G. designed, analyzed data, and wrote the manuscript. P.R. conceived the study and provided financial and administrative support. F.H. contributed with discussions. N.A., G.G, E.L.L., M.B., N.C., C.B., V.G., and J.P. performed and analyzed experiments.

ACKNOWLEDGMENTS

We are grateful to Montpellier Rio Imaging (MRI) for constructive microscopy; P. Fort and E. Andermacher for critical comments on the manuscript; C. Vincent, Y. Buscail, and N. Pirot for in vivo experiments (Animal facility and RHEM facility [Reseau d'histologie experimentale de Montpellier], respectively); and J.-C. Bourdon (University of Dundee, UK) for plasmids and helpful discussion. G.G., N.A., and P.R. are supported by Centre National de la Recherche Scientifique (CNRS) and Institut National de la Santé et de la Recherche Médicale (INSERM).

Received: July 7, 2014
Revised: February 3, 2015
Accepted: February 3, 2015
Published: March 5, 2015

REFERENCES

Aoubala, M., Murray-Zmijewski, F., Khoury, M.P., Fernandes, K., Perrier, S., Bernard, H., Prats, A.C., Lane, D.P., and Bourdon, J.C. (2011). p53 directly transactivates Δ133p53α, regulating cell fate outcome in response to DNA damage. Cell Death Differ. *18*, 248–258.

Bernard, H., Garmy-Susini, B., Ainaoui, N., Van Den Berghe, L., Peurichard, A., Javerzat, S., Bikfalvi, A., Lane, D.P., Bourdon, J.C., and Prats, A.C. (2013). The p53 isoform, Δ133p53α, stimulates angiogenesis and tumour progression. Oncogene *32*, 2150–2160.

Bieging, K.T., Mello, S.S., and Attardi, L.D. (2014). Unravelling mechanisms of p53-mediated tumour suppression. Nat. Rev. Cancer *14*, 359–370.

Bourdon, J.C. (2007). p53 and its isoforms in cancer. Br. J. Cancer *97*, 277–282.

Bourdon, J.C., Fernandes, K., Murray-Zmijewski, F., Liu, G., Diot, A., Xirodimas, D.P., Saville, M.K., and Lane, D.P. (2005). p53 isoforms can regulate p53 transcriptional activity. Genes Dev. *19*, 2122–2137.

Gadea, G., de Toledo, M., Anguille, C., and Roux, P. (2007). Loss of p53 promotes RhoA-ROCK-dependent cell migration and invasion in 3D matrices. J. Cell Biol. *178*, 23–30.

Hong, H., Takahashi, K., Ichisaka, T., Aoi, T., Kanagawa, O., Nakagawa, M., Okita, K., and Yamanaka, S. (2009). Suppression of induced pluripotent stem cell generation by the p53-p21 pathway. Nature *460*, 1132–1135.

Kawamura, T., Suzuki, J., Wang, Y.V., Menendez, S., Morera, L.B., Raya, A., Wahl, G.M., and Izpisúa Belmonte, J.C. (2009). Linking the p53 tumour suppressor pathway to somatic cell reprogramming. Nature *460*, 1140–1144.

Khoury, M.P., and Bourdon, J.C. (2011). p53 Isoforms: an intracellular microprocessor? Genes Cancer *2*, 453–465.

Liu, Y., Dong, Q.Z., Zhao, Y., Dong, X.J., Miao, Y., Dai, S.D., Yang, Z.Q., Zhang, D., Wang, Y., Li, Q.C., et al. (2009). P120-catenin isoforms 1A and 3A differently affect invasion and proliferation of lung cancer cells. Exp. Cell Res. *315*, 890–898.

Machado-Silva, A., Perrier, S., and Bourdon, J.C. (2010). p53 family members in cancer diagnosis and treatment. Semin. Cancer Biol. *20*, 57–62.

Figure 4. Chemotherapy Treatment of MCF-7 Breast Cancer Cells Upregulates Δ133p53 Isoform Expression and Activates Key Pluripotency Genes

(A) Western blot analysis of p53, p21, and C-MYC expression in MCF-7 cells after treatment with increasing doses of etoposide for 16 hr (DO1 antibody).

(B) The qRT-PCR analysis of *C-MYC* expression in MCF-7 cells upon treatment with increasing doses of etoposide (n = 4 independent experiments).

(C) The qRT-PCR analysis of Δ133p53 isoform expression in MCF-7 cells after etoposide treatment (n = 4 independent experiments).

(D) Western blot analysis of p53 isoform expression in MCF-7 cells after etoposide treatment (Sapu antibody).

(E) The qRT-PCR analysis of *SOX2*, *OCT3/4*, and *NANOG* expression in MCF-7 cells upon treatment with increasing doses of etoposide (n = 4 independent experiments).

(F) The qRT-PCR analysis of Δ133p53, *SOX2*, *OCT3/4*, and *NANOG* expression in control and MCF-7 cells transduced with Sh3 upon etoposide treatment (n = 4 independent experiments).

(G) Mammosphere quantification in MCF-7 cells transduced with Sh2 and treated with 50 ng/ml/day etoposide for 7 days (n = 3 independent experiments).

(H and I) The qRT-PCR analysis of *C-MYC*, *NANOG*, *OCT3/4*, and *SOX2* (H) and Δ133p53 isoform (I) expression in MCF-7 cells transduced with Sh2 and treated with 50 ng/ml/day etoposide for 7 days (n = 4 independent experiments).

Marcel, V., Petit, I., Murray-Zmijewski, F., Goullet de Rugy, T., Fernandes, K., Meuray, V., Diot, A., Lane, D.P., Aberdam, D., and Bourdon, J.C. (2012). Diverse p63 and p73 isoforms regulate Δ133p53 expression through modulation of the internal TP53 promoter activity. Cell Death Differ. *19*, 816–826.

Muller, P.A., Caswell, P.T., Doyle, B., Iwanicki, M.P., Tan, E.H., Karim, S., Lukashchuk, N., Gillespie, D.A., Ludwig, R.L., Gosselin, P., et al. (2009). Mutant p53 drives invasion by promoting integrin recycling. Cell *139*, 1327–1341.

Olivares-Illana, V., and Fåhraeus, R. (2010). p53 isoforms gain functions. Oncogene *29*, 5113–5119.

Roger, L., Jullien, L., Gire, V., and Roux, P. (2010). Gain of oncogenic function of p53 mutants regulates E-cadherin expression uncoupled from cell invasion in colon cancer cells. J. Cell Sci. *123*, 1295–1305.

Sarig, R., Rivlin, N., Brosh, R., Bornstein, C., Kamer, I., Ezra, O., Molchadsky, A., Goldfinger, N., Brenner, O., and Rotter, V. (2010). Mutant p53 facilitates somatic cell reprogramming and augments the malignant potential of reprogrammed cells. J. Exp. Med. *207*, 2127–2140.

Terrier, O., Josset, L., Textoris, J., Marcel, V., Cartet, G., Ferraris, O., N'guyen, C., Lina, B., Diaz, J.J., Bourdon, J.C., and Rosa-Calatrava, M. (2011). Cellular transcriptional profiling in human lung epithelial cells infected by different subtypes of influenza A viruses reveals an overall down-regulation of the host p53 pathway. Virol. J. *8*, 285.

Terrier, O., Marcel, V., Cartet, G., Lane, D.P., Lina, B., Rosa-Calatrava, M., and Bourdon, J.C. (2012). Influenza A viruses control expression of proviral human p53 isoforms p53β and Delta133p53α. J. Virol. *86*, 8452–8460.

Ungewitter, E., and Scrable, H. (2010). Delta40p53 controls the switch from pluripotency to differentiation by regulating IGF signaling in ESCs. Genes Dev. *24*, 2408–2419.

Utikal, J., Polo, J.M., Stadtfeld, M., Maherali, N., Kulalert, W., Walsh, R.M., Khalil, A., Rheinwald, J.G., and Hochedlinger, K. (2009). Immortalization eliminates a roadblock during cellular reprogramming into iPS cells. Nature *460*, 1145–1148.

Vinot, S., Anguille, C., de Toledo, M., Gadea, G., and Roux, P. (2008). Analysis of cell migration and its regulation by Rho GTPases and p53 in a three-dimensional environment. Methods Enzymol. *439*, 413–424.